ORIGINAL PAPER

Modal identification of concrete dams under natural excitation

Sérgio Pereira[1] · Filipe Magalhães[1] · Álvaro Cunha[1] · Carlos Moutinho[1] · João Pacheco[1]

Abstract

Historically, the dynamic testing of concrete dams has been associated with experimental modal analysis (EMA) and the performance of forced vibrations tests. Nevertheless, this type of tests requires the use of a heavy equipment and the interruption of the regular operation of the structure. An alternative to EMA relies on the application of operational modal analysis (OMA), through the performance of ambient vibration tests, and thus, it is essential to investigate if the application of OMA to concrete dams can provide good results with high levels of accuracy. In this context, this work addresses the performance of ambient vibration tests on concrete dams with quite diverse geometrical attributes and on the application of state-of-art output-only modal identification methods, to gain awareness of the issues that may occur during the application of OMA methods to signals with such low amplitudes (of the order of micro g), such as those that are usually recorded when dealing with these massive structures. More specifically, the paper describes the ambient vibration tests executed on six very different concrete dams. The most relevant modal properties are estimated through the application of modern output-only modal identification techniques, stressing the good level of accuracy achieved, which is quantified through the calculation of modal properties' uncertainties. Finally, a novel approach considering the uncertainties estimated is used to study the effect of noise on the quality of modal estimates and to qualify the adequacy of sensors to perform these tests on dams.

Keywords Operational modal analysis · Concrete dams · Ambient vibration tests · Noise levels

1 Introduction

Classically, forced vibration tests have been used to identify the dynamic properties of structures for numerical modelling (or design) updating and validation [1–5]. The application of an experimental modal analysis by performing forced vibration tests is an effective and rigorous mean of defining the modal properties of a civil engineering structure. This methodology has been successively employed on dams in the past, as well as on bridges [6] and buildings [7]. Nevertheless, this procedure shows a few disadvantages, since for bridges, and for dams crossed by roads, on one hand, traffic must be interrupted to perform the test, and on the other, the dimensions and weight of the equipment that needs to be used to excite these enormous structures may rise conveyance issues [8].

Notwithstanding, the technological progression that occurred in the area of data acquisition during the past few decades contributed significantly to the dissemination of ambient vibration tests as a reliable alternative. These functional tests allow to carefully identify the modal properties of civil engineering structures with no need to disturb their normal service conditions. Besides, the modal properties are extracted from data acquired under normal operation conditions, instead of artificially created excitation. The successful application of operational modal analysis has already been verified in many different examples of civil engineering structures, such as cable-stayed bridges [9], suspension bridges [10], footbridges [11], viaducts [12], stadia roofs [13], towers [14], wind turbines [15], buildings and infill walls [16, 17], or even nuclear power plants [18]. Ambient vibration tests are often performed, prior to rehabilitation activities to study and to better understand the structure, after the construction of essential infrastructures to validate numerical models or even as part of inspection plans to assess the safety of structures already built. Moreover, the information yielded by operational modal analysis can be used in the definition of dynamic monitoring systems [19]

✉ Sérgio Pereira
  sbp@fe.up.pt

1   Construct-ViBest, Faculty of Engineering (FEUP),
    University of Porto, Rua Dr. Roberto Frias, 4200-465 Porto,
    Portugal

for the shaping and tuning of devices directed to the control of vibrations.

Given that when conducting an ambient vibration test, the vibrations registered are not caused by any artificial source specifically prepared for the test, but to the surrounding ambience or to nearby human activity, the vibration levels detected are usually relatively lower than the ones that are typically verified when forced vibrations are used, leading to the necessity of employing superior equipment during the test, namely sensors and data acquisition system. Nonetheless, the testing of more flexible structures such as towers or pedestrian bridges, which are easier to excite, may proportionate good results, even using equipment of lower quality.

For instance, when testing concrete dams, it usually should be expected to measure low vibration levels [20], given the massive nature of these structures and the isolated locations where many of them are positioned, so superior equipment is needed to perform successful experimental campaigns. Nevertheless, the dynamic testing of concrete dams based on the recording of ambient-induced vibrations has been carried out before [21–25] quite often as a supplement to forced vibration campaigns. Recently, the execution of these tests on dams to correct numerical models and to corroborate structural assumptions became more common [26–29], prompting the implementation of structural health monitoring systems based on the recording of vibrations that rely entirely in environmental excitation and on dependable measuring and acquisition equipment [30, 31].

Nevertheless, top-quality equipment may not always be available, given that it usually represents high costs. Therefore, in certain situations, low-cost options, with not so high potentialities, can emerge as an alternative solution. In this sense, when performing operational modal analysis, it is essential to examine the accuracy of the outcomes reached with accelerometers with a broad range of potentialities [32].

Therefore, the present work addresses the ambient vibration testing of a set of concrete dams with diverse structural profiles, which had the purpose of identifying the issues related to the low intensity of the signals recorded through the execution of ambient vibration tests on dams, and studying the quality of the results that can be attained with these type of application (Fig. 1).

In the following sections, details are presented about the tests performed in Alto Lindoso, Bouçã, and Castelo do Bode dams. Estimates are obtained for the modal properties of the tested dams and the uncertainty associated with these properties. A summarized set of results is presented for the tests performed in Caldeirão, Santa Luzia, and Aguieira dams.

Finally, the time-series of accelerations recorded at Alto Lindoso and Bouçã arch dams are numerically adulterated with growing degrees of noise to simulate that different accelerometers were used during the tests, instead of the force-balance accelerometers that were actually used. The results obtained with real experimental data and with simulated data and studied and compared.

2 Experimental procedure and equipment

Unlike forced vibration tests, which require the use of shakers or instrumented hammers, during ambient vibration tests, there is neither the need to excite the structure artificially nor to measure the input action that is causing the structure to vibrate, rendering a relatively simple experimental procedure [Santos, 34]. Therefore, ambient vibration testing roughly consists of recording the vibrations on a structure that is subjected to anything else than ambient noise. For this, a combination of reference sensors and moving sensors can be used, noting that the first remain fixed at their positions, while the latter may be placed at various locations during the test.

When preparing a dynamic test, it is crucial to have in mind that the spatial precision required to determine the mode shapes of the structure correctly plays an essential role in the definition of the number of points to instrument during the test. For this, and to guarantee that reference points are positioned away from nodal points, it is vital to predicting the mode shapes of the structure, prior to the execution of the test, for which the consideration of similar structures and the analysis of numerical models are of good help. Moreover, the distribution of sensors as references or moving sensors rests on the number of sensors accessible to execute the test and on the size of the structure tested. For instance, if the quantity of sensors available is smaller than the number of points to cover, at least one sensor must be used as a reference, though it is advisable to use more than one reference point. When testing smaller structures and the number of sensors available is not a limitation, it is desirable to perform the test using all the points as fixed sensors (references), since this will simplify data processing.

In terms of data acquisition, it is vital that the dimension of the time-series recorded and the sampling rate selected to record them are chosen carefully, since the volume and quality of the data available largely depends on these two factors. In the case of the sampling frequency, the value to adopt can be limited either by the attributes of the equipment used or by the dynamic properties of the structure under study. So that aliasing errors can be effectively avoided [35], the sampling rate should be greater than at least two times the highest frequency captured by the accelerometers or than the cutting frequency of analogue low-pass filters that may exist in the measuring chain. In addition, the total of vibration modes to be determined will be limited by the sampling rate, since it will only be possible to detect frequencies lower than

Fig. 1 Pictures of the tested dams [33]

1 - Alto Lindoso dam (crown length: 110m; height: 297m)

2 - Caldeirão dam (crown length: 122m; heigth: 39m)

3 - Santa Luzia dam (crown length: 178m; height: 76m)

4 - Bouçã dam (crown length: 175m; heigth: 63m)

5 - Castelo do Bode dam (length: 402m; heigth: 115m)

6 - Aguieira dam (crown length: 400m; heigth: 89m)

half of this parameter's value, and so it should be adopted accordingly.

Furthermore, the quality of the modal parameters' estimation depends on the length of the time-series recorded in each setup, which impacts, in particular, the estimation of damping estimates. To choose the best length for the time-series, a few points should be considered such as the structure's first frequency, the values of damping, the ratio between signal and noise intensities, and also the method used to perform the identification of modal properties (parametric methods can improve the quality of the results) [36]. For this reason, the optimal time length varies with the structure studied and with the equipment available to perform the experiment. A rule proposing that time-series as long as 1000–2000 times the value of the first frequency's period should be acquired can be found in [37], though reliable outcomes can be achieved with relatively shorter lengths (more than five times shorter), as presented by [36]. Time-series

with extensions between 15 and 60 min have been used in the experimental campaigns presented in this work, corresponding to lengths from 1800 to 7200 times the period of the respective structure's first frequency.

Systems used to perform measurements and to record data during experimental campaigns are composed of many elements, the most important of which are probably the sensors. Accelerometers are the most common type of sensor used to test civil engineering structures, and force-balance accelerometers are the adequate type of accelerometer to test them. However, another type of sensors measuring, for instance, displacements, velocities, or strains are also common and alternative types of accelerometers, with various working operational basis, such as piezoelectric, MicroElectroMechanical or capacitive, can be used as well. Force-balance accelerometers start measuring at DC, which means that they can detect the lowest frequencies (as an example, in [38] a tower's fundamental frequency of just 0.35 Hz is

detected using force-balance accelerometers). In addition, these sensors are particularly suited to the testing of deficiently excited structures, such as remotely located concrete dams, since they have high sensitivity and low noise.

Generally, sensors produce continuous electrical signals that are then transformed in analogue-to-digital converters to the discrete signals that are saved in computers. The most relevant property of these converters is the number of bits, since the resolution of the measurement roughly corresponds to the division of the measuring range by two to the power of the number of bits. Therefore, it is worth noting that even if the best sensors are used to perform a measurement, the quality of the digital signal (which will be used to process the data) can be compromised if low-quality analogue-to-digital converters are used to transform the signal. Besides the mentioned elements, low-pass filters or signal amplifiers may be included in the acquisition chain as well to enhance the quality of the digital signal. Furthermore, data processing methods can be used to try to improve the quality of the identification reducing the impact of noise [39].

Experimental tests may either resort to centralized schemes, where the signal produced in each sensor is transferred through electrical cables to a single data acquisition system, and all signals are converted to digital form at this point or to autonomous portable recorders where measuring and conversion occur in the same device, and digital signals are then put together in a computer. Examples of both types of acquisition systems are presented in Fig. 2. These portable recorders consist of tri-axial force-balance accelerometers, that may be located in the interior or in the exterior of the recorder, an analogue-to-digital converter with 24 bits, a flashcard enable the direct download of the recorded data to a computer, and a rechargeable battery that provides energy for many hours. Prior to the test, the recorders parameters must be set up according to the test plan and recording characteristics intended. The synchronization between devices is assured through GPS.

Based on the characteristics of each dam, the experimental campaigns addressed in this work were executed resorting to the portable recording devices or the central acquisition system, according to the pros and cons of each system. For instance, the centralized system used has a range limit of about 150 m, while the portable devices can only be used outside, due to the need of having a GPS signal.

3 Data processing and noise simulation

The data recorded during ambient vibration tests should first be pre-processed, which may include the elimination of offsets, filtering, resampling, and storage. After this, output-only identification algorithms [40, 41] can be used to obtain the modal properties of the structure, which can provide accurate results even if the excitation is not a stationary white noise [42]. In the present work, the peak-picking (PP) [43] and the covariance-driven stochastic subspace identification (SSI-Cov) [44] methods are used.

The peak-picking is a basic identification method, with a few drawbacks, but very helpful for an expeditious analysis of the data. In turn, the SSI-Cov is a robust and stable method, though its application is more time-consuming. Therefore, the sequential application of these methods to accelerations time-series recorded in a structure results in a stable procedure that produces reliable results. In addition, to better understand the accuracy achieved with the identification, a variant of the SSI-Cov method is used that was first introduced by [45] and then computationally improved by [46], which provides the possibility of estimating the uncertainty associated with the identified modal properties and allows to enhance the efficiency of automatic operational modal analysis [47]. Stabilization diagrams are used to help distinguish between real and spurious modes [48].

To enrich the study developed around the data recorded during the experimental campaigns that were carried out, an investigation is conducted to determine the feasibility of using accelerometers with other functioning principles than force-balance (FB). For this, the noise floors that may be expected for regular piezoelectric (P) and MicroElectrical-Mechanical (MEMS) [49] accelerometers were established. Laboratory experiments were performed on two piezoelectric accelerometers (PE1 and PE2), and two MicroElectrical-Mechanical accelerometers (MEMS 1 and MEMS 2), representing sensors with medium and high quality, respectively.

Fig. 2 On the left: centralized acquisition system with cables; on the right: portable recorder with GPS antenna

In all the studied cases, noise floors were constant in the frequency range under analysis.

The spectral noise levels of the studied accelerometers were evaluated in a laboratory environment and then simulated through the numerical generation of white noise time-series, which are presented in Fig. 3. It should be noted that considering the logarithmic nature of the vertical scale in Fig. 3, the difference in quality between MEMS and piezoelectric is evident. The two studied piezoelectric accelerometers show a noise floor below 10^{-11} [g^2/Hz], yet for MEMS, these values are approximately 10^{-9} and 10^{-10} [g^2/Hz].

In addition, Fig. 4 presents accelerations recorded in the central measuring point of each of the tested dams, when the respective power plants were not operating, so that vibration levels can be compared. The exception is Castelo do Bode dam whose turbines operated during the entire test. The levels of vibration verified vary from tens of micro g, either when human works using heavy machines occur in the surroundings or when the dam is crossed by traffic to just a few micro g in calm conditions.

The auto-spectra obtained with the signals displayed in Fig. 4 are presented in Fig. 5, exposing the minimum signal amplitude that allows to adequately characterize the auto-spectra observed in all the dams tested, which is between 10^{-13} and 10^{-14} g^2/Hz.

Comparing Fig. 3 with Fig. 5, it becomes clear that when using MicroElectricalMechanical accelerometers to perform ambient vibration tests on dams, it is likely that only noise will be recorded. This is further analysed in the next few sections.

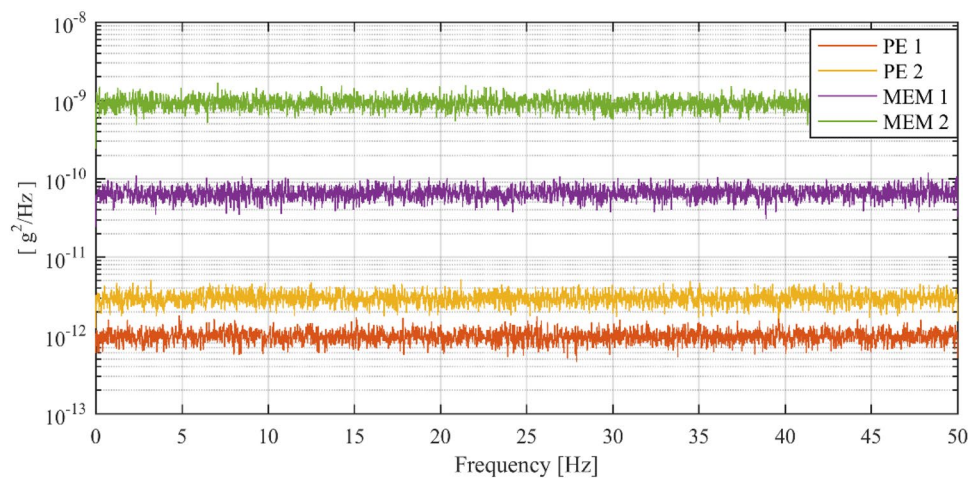**Fig. 3** Noise spectra numerically generated

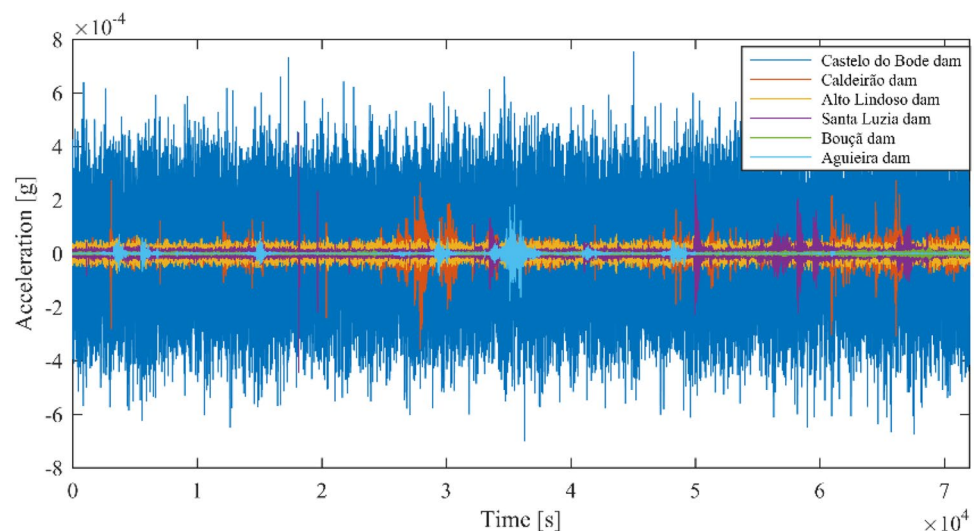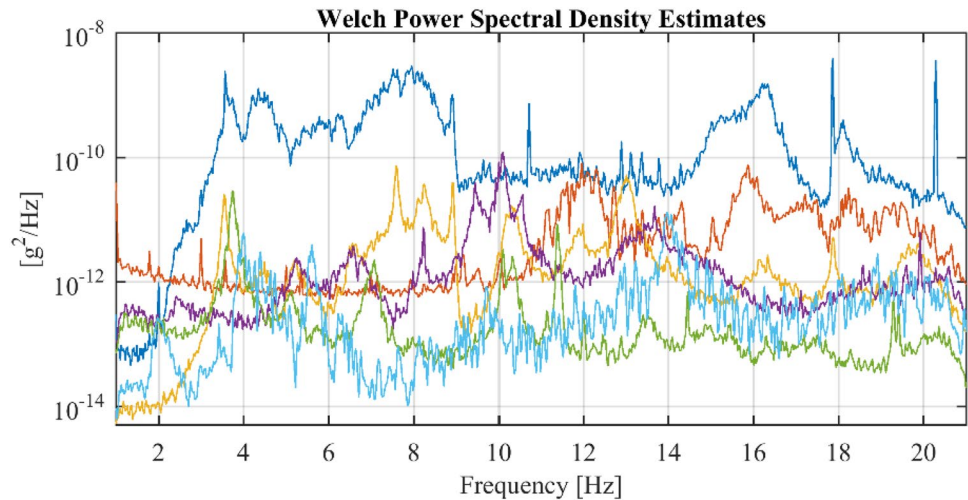**Fig. 4** Time-series of accelerations recorder in the six dams tested

4 Alto Lindoso dam

4.1 Description of the dam and ambient vibration test

Alto Lindoso is an arch dam with double curvature integrated into a tight canyon located in the north of Portugal (see Fig. 6), which started operating in 1992 [33]. This 110-m high concrete dam has a 297-m long crest which embodies a connection over the two margins of Lima River. The respective power plant is less than 100 m afar from the dam and the two vertical Francis turbines operating in the plant (214.3 rpm–3.57 Hz) represent an installed capacity of 630 MW.

An ambient vibration test was performed on Alto Lindoso dam on the 22nd of February 2017, for which ten recorders with tri-axial force-balance accelerometers were used, though only the radial direction was recorded. Given the dam's substantial scale, a test layout contemplating 21 recording positions was prepared, with one measuring point for each of the 21 concrete blocks of the dam. The defined test grid was covered over four measuring setups during which four accelerometers acted as moving sensors, while other six accelerometers were used as references throughout the entire test. The reference points were marked in Fig. 7 with red dots, whilst blue dots were used to mark the 15 points covered by moving sensors.

The full test took 4 h, divided into four setups of 58 min, separated by 2-min intervals used for sensor repositioning. The data acquisition was realized with a sampling rate of
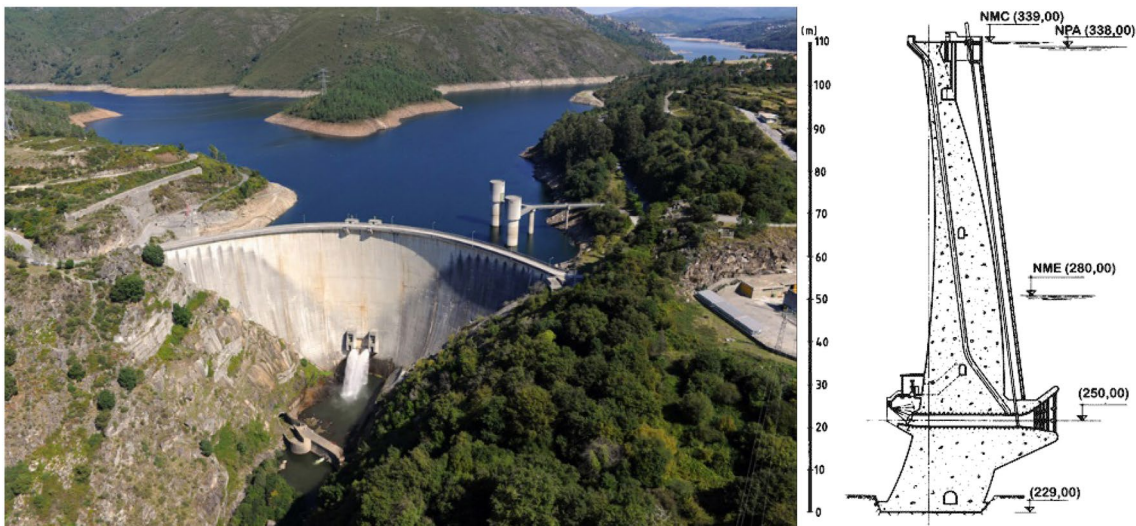

Fig. 6 Frontal picture [33] and a scheme of cross section [50] from Alto Lindoso dam

100 Hz that was then adjusted to half of that through decimation (50 Hz). During the test, a level of water of 322 m was verified.

4.2 Modal properties' identification

The identification process starts with the employment of the Peak-Picking method which, though not very accurate, allows to achieve rough estimates of the most relevant natural frequencies in an expeditious manner.

Figure 8 presents the averaged and normalized power spectral density function (ANPSD) that was obtained with the application of this method, where the identified vibration modes and respective peaks are highlighted with orange circles. Then, to achieve natural frequency estimates and mode shapes with higher accuracy, the SSI-Cov method was applied, which allows as well to identify damping values. Model orders between 20 and 90 were considered during the application of SSI-Cov to each measured setup.

Figure 9 presents the stabilization diagram obtained from the third setup, where vertical alignments of poles

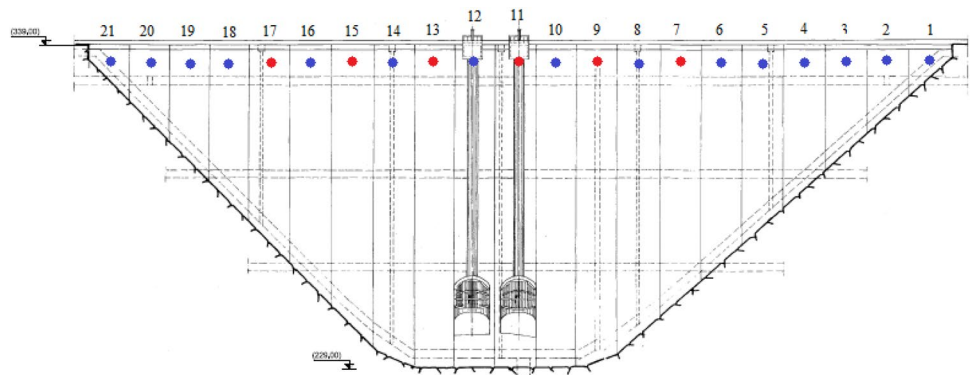**Fig. 7** Alto Lindoso dam: test layout

Fig. 8 Alto Lindoso dam: averaged normalized power spectral density function
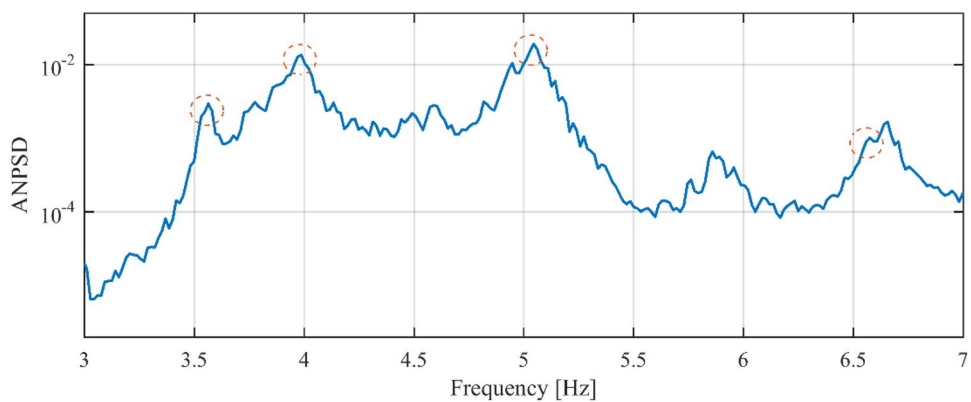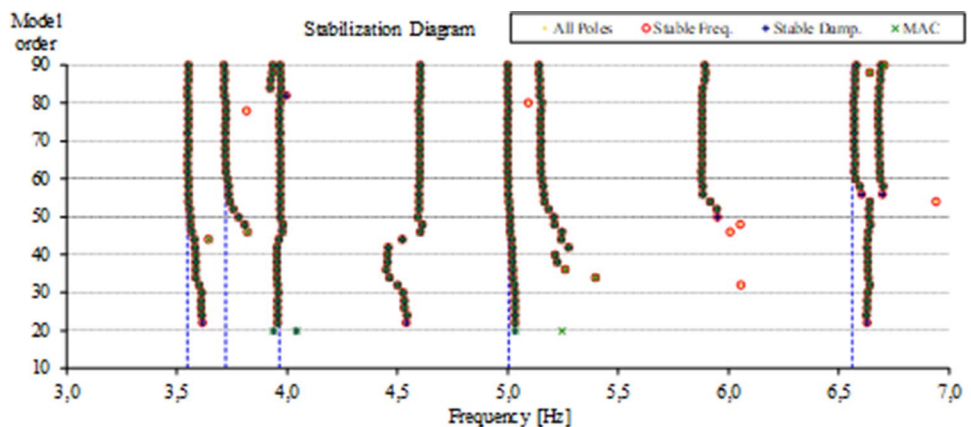

Fig. 9 Alto Lindoso arch dam: stabilization diagram

are clearly distinguished, and blue dashed lines point to the alignments determine as being associated with vibration modes of the structure.

In addition, it is relevant to note that the entire set of peaks and alignments observed, respectively, in the power spectral density function and the stabilization diagram were investigated, which included the analysis of the shapes of the modal configurations resulting from all of them. The group of identified vibration modes settled at the end of the analysis corresponds to the ones that were achieved simultaneously through the two identification methods, and that presented reasonable mode shapes, as well.

The first four modes of vibration of the dam were determined, and Table 1 presents values for their modal properties and the description of their modal configurations. Since four setups were needed to perform the test, the values here presented represent the averaging of the results from stable poles in the stabilization diagrams of each setup. It is worth noting that two distinct frequencies are related to the first symmetric vibration mode (designated as modes 2a and 2b), since quite different frequency values were obtained for the different levels of vibration verified during the test.

The standard deviation values related to the estimates of model properties (i.e., natural frequencies and damping ratios) are presented in Table 1 as well, giving extra insight into the accuracy achieved with the identification. For instance, for Alto Lindoso dam, modes one and four (both antisymmetric) present the smaller values for the standard deviation of both frequency and damping estimates, respectively, below 0.01 Hz and 0.2%. On the other hand, the other two modes (both symmetric) present standard deviations' estimates that, though acceptable, are significantly higher.

Figure 10 presents the well-delimited and coherent modal configurations that were obtained for the four vibration modes determined. While modes one and four present antisymmetric shapes, modes two and three show nearly symmetric ones.

In 1992, a forced vibration test was realized in Alto Lindoso Dam [51]. During this test, the level of water in the reservoir was 326 m above sea level, which represents operational conditions close to those verified during the performance of the ambient vibration test in 2017, when the water level was about 4 m below. A numerical model was also developed back in 1992 to compare numerical and experimental results [51].

In the numerical model presented the material constituting the dam is assumed to have an elastic behaviour, the rock mass foundation was assumed as elastic isotropic. In turn, for simplification, the foundation was considered to be massless, and the water in the reservoir was modelled through the addition of Westergaard masses [52]. To compare the results obtained, Table 2 presents the natural frequencies achieved through the experimental tests performed in 1992 and 2017, together with the ones obtained with the numerical model built in 1992, and a good agreement is verified between the modal properties obtained from the three mentioned sources.

4.3 Noise simulation

The spectra resulting from the time-series recorded in Alto Lindoso dam and the spectra of the noises previously simulated and presented in Fig. 3 are compared in this section. Subsequently, the time-series of noises that were numerically simulated are combined with the measured data, and a comparison is made between the results achieved with the studied scenarios (MEMS1, MEMS2, PE1, PE2, and FB).

The mentioned noise floors are analysed together with auto-spectra resulting from experimental data recorded with two sensors that were in separate points, while the field-testing campaign took place. These spectra are presented in sub-sections (a) and (b) of Fig. 11. Considering the noise floors related to piezoelectric sensors, it should be noted that even if PE1 is permanently under the peaks of the experimental spectra, in turn, PE2 is under many peaks, but sporadically overpassing some peaks. On the other hand, the contrary is verified with MEMS, given that MEMS2 is permanently above the peaks, while MEMS1 either stands through the peaks or above the peaks.

Finally, data simulating band-limited white noise were mixed with experimental time-series of accelerations recorded on-site, considering constant spectral noise over the frequency range that is being analysed. New time-series were obtained through the addition of the ones containing noise to the experimental measurements, thus simulating the outcomes that would have been recorded in the case that piezoelectric (or MEMS) accelerometers had been used during the experimental campaign.

Table 1 Modal properties of Alto Lindoso

Mode order	f_{mean}[Hz]	f_{std}[Hz]	ξ_{mean}[%]	ξ_{std}[%]	Mode shape description
1st	3.5460	0.0045	1.190	0.120	Antisymmetric
2nd a	3.7520	0.0257	2.850	0.690	Symmetric
2nd b	3.9630	0.0105	2.160	0.280	Symmetric
3rd	5.0080	0.0170	1.590	0.360	Symmetric
4th	6.5630	0.0094	1.310	0.170	Antisymmetric

Fig. 10 Mode shapes of Alto Lindoso arch dam first four vibration modes

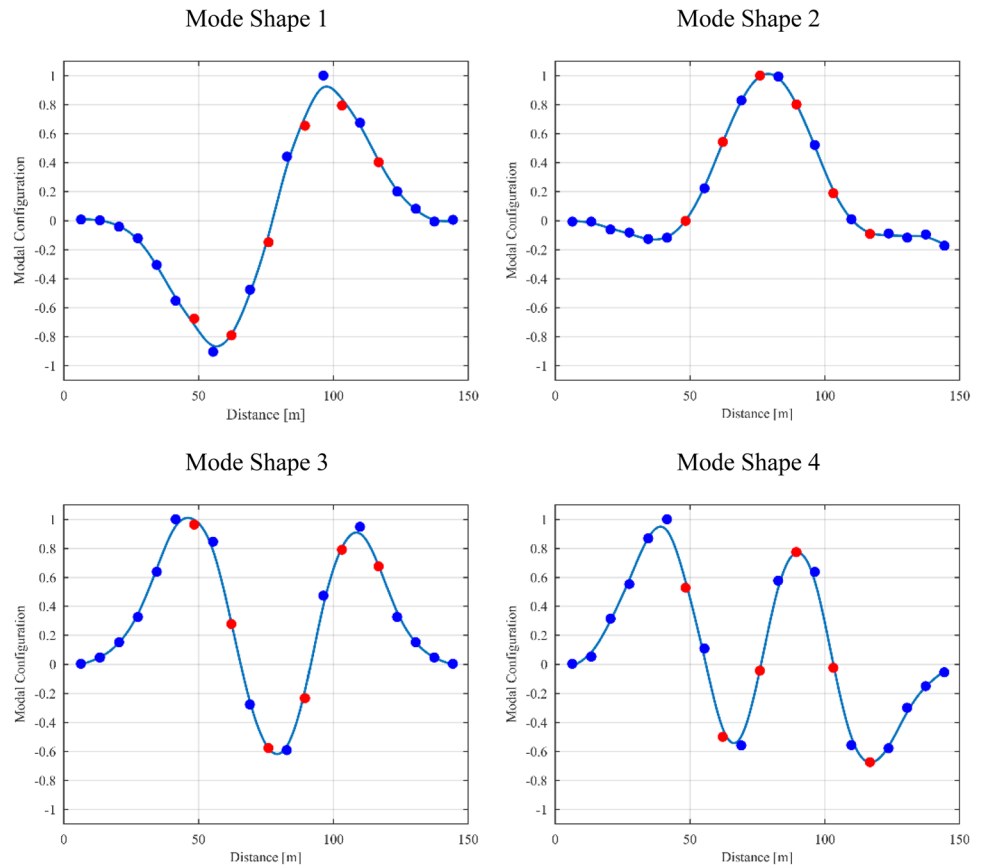Mode Shape 1

Mode Shape 2

Mode Shape 3

Mode Shape 4

Table 2 Comparison between the natural frequencies obtained with the experimental and numerical works developed in 1992 and 2017

Mode	Ambient vibration test 2017 [Hz]	Forced vibration test 1992 [Hz]	Numerical model 1992 [Hz]
1st	3.55	3.45	3.43
2nd	3.75/3.96	3.80	3.93
3rd	5.01	5.30	5.03
4th	6.56	6.60	6.51

Subsections (c) and (d) of Fig. 11 show auto-spectra obtained with experimental data that was actually recorded on-site with the force-balance accelerometers (in blue) and with data simulating piezoelectric and MEMS-based recordings. Most of the peaks in the spectra obtained from the experimental data (FB) appear as well in the results from the analysis of the piezoelectric simulations (PE1 and PE2), which is not verified with the results extracted from the MEMS' simulated data. In this last case, many time-series result in spectra where the peaks are hidden below the noise floor.

Through the application of the SSI-Cov method, automatic modal identification was performed, first using the experimental data obtained during the test (FB) and then the other four sets of time-series which resulted from the combination of experimental data with numerically simulated noises. Modal properties were identified for the entire set of time-series, including each mode's natural frequency, damping ratio, and the standard deviations of the previous estimates.

Modal properties' estimates obtained for the five cases under study are presented in Table 3, including average and standard deviation values of vibrations modes number one and two. Analysing either natural frequencies or damping ratios, it is verified that the values of standard deviations related to these parameters rise parallelly to the intensity of the noise added to the experimental data, even if, for the two piezoelectric cases (PE1 and PE2), just minor result variations are observable, comparing these with the original results. On the other hand, significant changes occur with the results determined from data simulating MEMS measurements, with much higher uncertainties being identified. It is worth noticing that the first mode was not even identified when using MEMS2 time-series, which is also verified with higher order modes.

Fig. 11 **a**, **b**: Auto-spectra from experimental data (blue) and auto-spectra from noise floors numerically generated; **c**, **d**: auto-spectra from experimental data adulterated with numerically generated noises

(a)

(b)

(c)

(d)
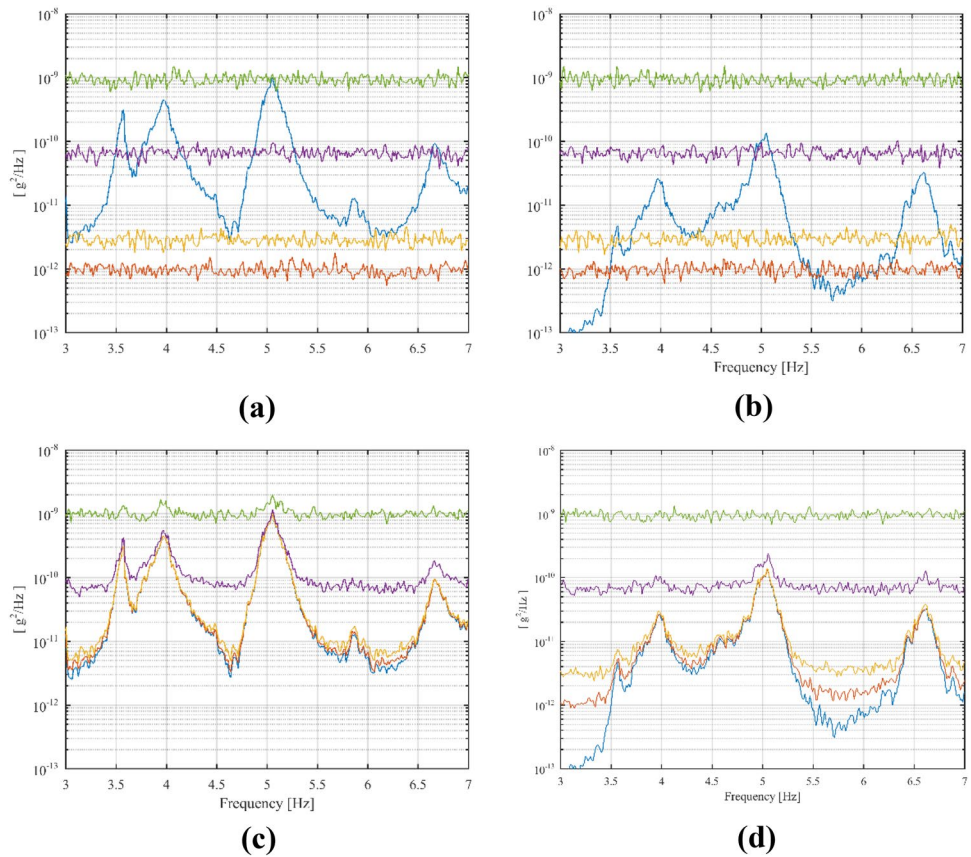
5 Bouçã dam

5.1 Description of the dam and ambient vibration test

Table 3 Natural frequencies, damping ratios, and corresponding standard deviations for the first two vibration modes of Alto Lindoso dam

Scenario	f_{mean}[Hz]	f_{std}[Hz]	ξ_{mean}[%]	ξ_{std} [%]
Mode 1				
FB	3.5460	0.0045	1.194	0.123
PE1	3.5460	0.0046	1.278	0.136
PE2	3.5450	0.0064	1.054	0.212
MEMS1	3.5630	0.0165	1.340	0.457
MEMS2	–	–	–	–
Mode 2				
FB	3.9630	0.0105	2.164	0.280
PE1	3.9620	0.0106	2.159	0.280
PE2	3.9640	0.0106	2.139	0.284
MEMS1	3.9600	0.0175	2.375	0.466
MEMS2	3.9470	0.0302	2.084	0.708

The Bouçã dam is a concrete double arch dam located in Pedrogrão Grande, Portugal, whose reservoir is accomplished with water from the Zêzere River. The 63-m-high and 175-m-long dam is operating since 1955 when two Francis turbines operating at 214.3 rpm (3.57 Hz) were installed in the hydroelectric plant that lays downstream from the dam. An aerial picture of the dam is presented in Fig. 12, side-by-side with a scheme of the cross section.

On the 12th of June 2018, an ambient vibration test was realized on Bouçã dam. To perform the test, nine force-balance accelerometers were positioned on the first visit gallery of the dam, which were fixed in the same position during the entire test. The nine sensors were connected to a central acquisition station through cables, but the farthest one was only 65 m away.

Nine measuring points were used, so that each sensor were positioned in the middle of each of the dam's nine interior blocks, corresponding to the part of the dam where the spillway is located. The test layout is presented in Fig. 13 using a scheme of the structure and blue dots to point the position of each measuring point.

The test consisted of five recording setups, each of them with 13 min of duration, and the data acquisition was performed with a sampling rate of 100 Hz (reduced to 50 Hz during pre-processing). The elevation of the water in the

reservoir throughout the experimental procedures was constant at 174.7 m.

5.2 Identification of modal properties

The procedure used in the previous section to identify the modal properties of Alto Lindoso dam was repeated, once again using the Peak-Picking method to obtain a first set of natural frequencies expeditiously. In Fig. 14, orange circles

were used to highlight the peaks of the ANPSD function that were identified as being associated with vibration modes. The first vibration mode of the dam was identified with a frequency close to 3.30 Hz, but a significant number of other peaks appear between 3 and 12 Hz.

The SSI-Cov method was used afterwards to corroborate the preliminary analysis and to achieve a more accurate group of modal properties estimates, for which model orders between 20 and 80 were used. With the
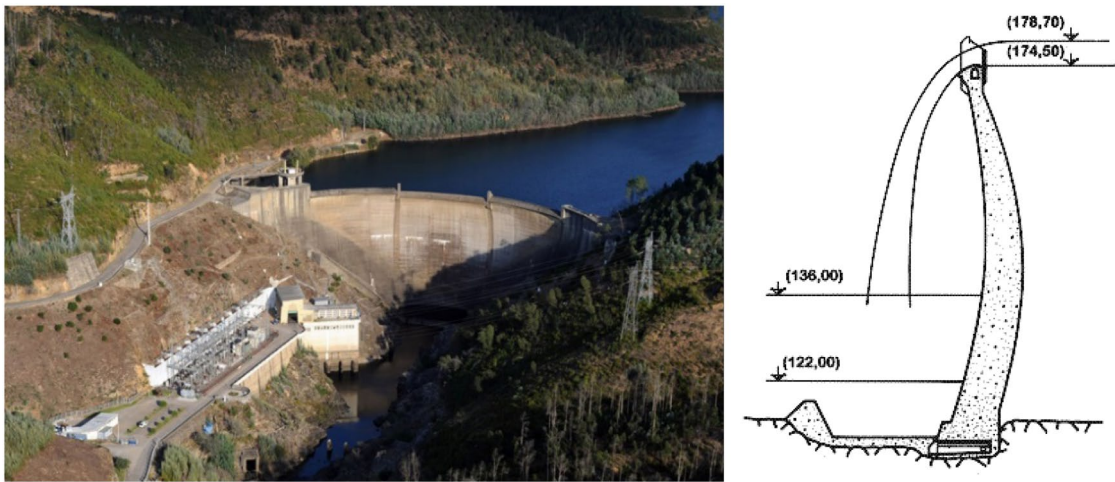

Fig. 12 Aerial view [33] and cross section [50] of Bouçã dam

Fig. 13 Test layout of the ambient vibration test performed on Bouçã dam
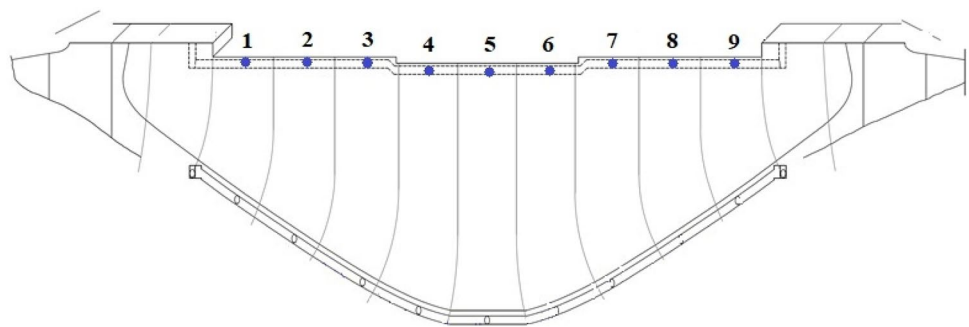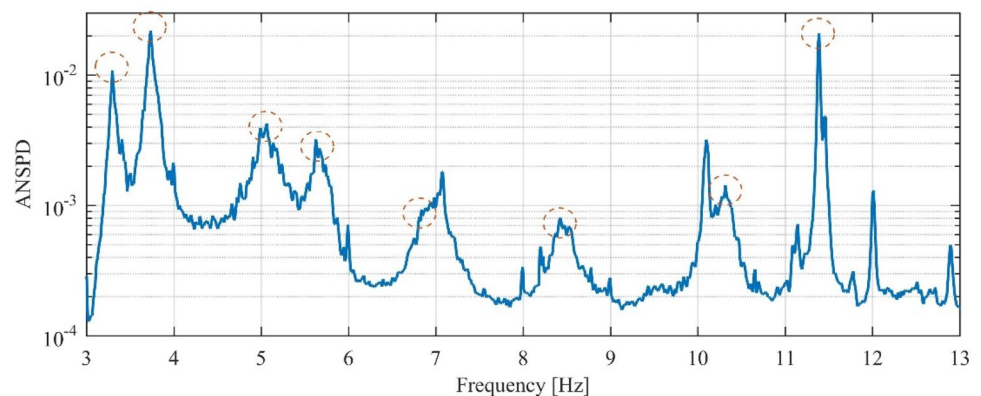

Fig. 14 ANPSD function obtained from data recorded during the experimental campaign carried out at Bouçã dam, with orange circles highlighting the identified vibration modes

Springer

application of the SSI-Cov method to the recorded data, similar results were achieved through all the setups. The stabilization diagram that resulted from the application of this method to the experimental data measured during the third setup is presented in Fig. 15, where precise alignments of poles are observable. Blue lines mark the alignments associated with the vibration modes of the dam.

Table 4 presents the modal properties of the eight vibration modes that were identified.

Regarding the uncertainties associated with modal properties, it can be noted that smallest standard deviation values are related to the first two vibration modes, whereas the third vibration mode, whose identification was not achieved for the whole set of analysed setups, seem to present the less accurate estimates, showing the highest values for the standard deviations of the modal properties.

Figure 16 presents the modal configurations that were obtained for the eight vibration modes determined, being all of them well characterized. The first two vibration modes are, respectively, antisymmetric and symmetric, similar to what was verified with Alto Lindoso dam. Finally, alternate states of symmetry are found in the configurations of modes 3–8.

5.3 Noise simulation

The procedure presented in Sect. 4.3 is repeated, now using data recorded at Bouçã dam to compare the auto-spectra resulting from measured data (FB) with the simulated noise floors associated with piezoelectric (PE1 and PE2) and MEMS (MEMS1 and MEMS2) sensors that were previously defined. This comparison is presented in Fig. 17a.

Unlike what was observed for Alto Lindoso dam, in the case of the test performed in Bouçã dam, no relevant amplitude variations are verified between spectra obtained from data measured in different positions during the same setup, which can be explained by the shorter length of the crown at Bouçã dam and by the fact that the measuring grid is concentrated in the central part of the dam, reasonably distant from the abutments.

In this case, while the noise floors used to simulate piezoelectric sensors (PE1 and PE2) are either above or crossing the peaks of the spectra obtained from real data, the two spectra simulating MEMS are permanently over such peaks. The procedure consisting of adding the original recordings of accelerations to the data simulating band-limited white noises was repeated, assuming a constant spectral noise inside the studied interval of frequencies. Therefore, time-series of accelerations simulating the dynamic testing of Bouçã dam using piezoelectric and MEMS accelerometers were obtained.

Fig. 15 Stabilization diagram obtained from the application of the SSI-Cov method to data recorded during the ambient vibration test performed at Bouçã dam, with blue lines highlighting the identified vibration modes
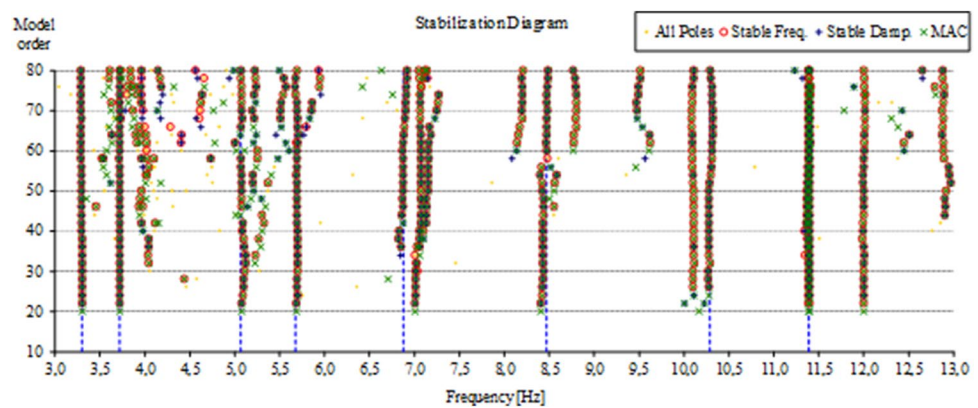

Table 4 Modal properties of Bouçã dam

Mode order	f_{mean}[Hz]	f_{std}[Hz]	ξ_{mean}[%]	ξ_{std} [%]	Mode shape description
1st	3.296	0.0069	1.464	0.206	Antisymmetric
2nd	3.733	0.0058	1.308	0.161	Symmetric
3rd	5.074	0.0342	3.203	0.605	Symmetric
4th	5.676	0.0169	1.816	0.298	Antisymmetric
5th	6.875	0.0342	1.782	0.504	Symmetric
6th	8.452	0.0204	1.566	0.254	Antisymmetric
7th	10.289	0.0236	0.999	0.256	Symmetric
8th	11.394	0.0336	1.942	0.486	Antisymmetric

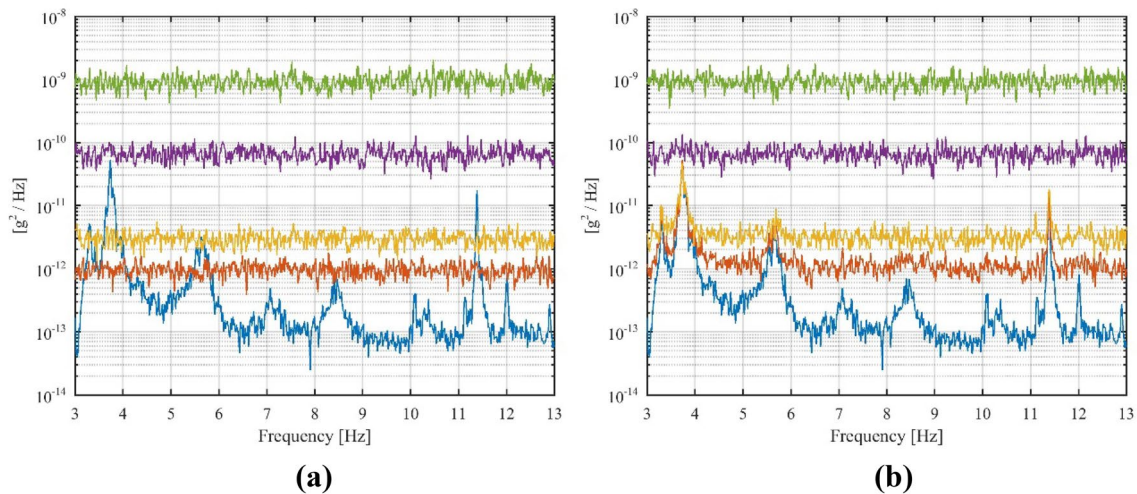**Fig. 16** Mode shapes of Bouçã arch dam first eight vibration modes
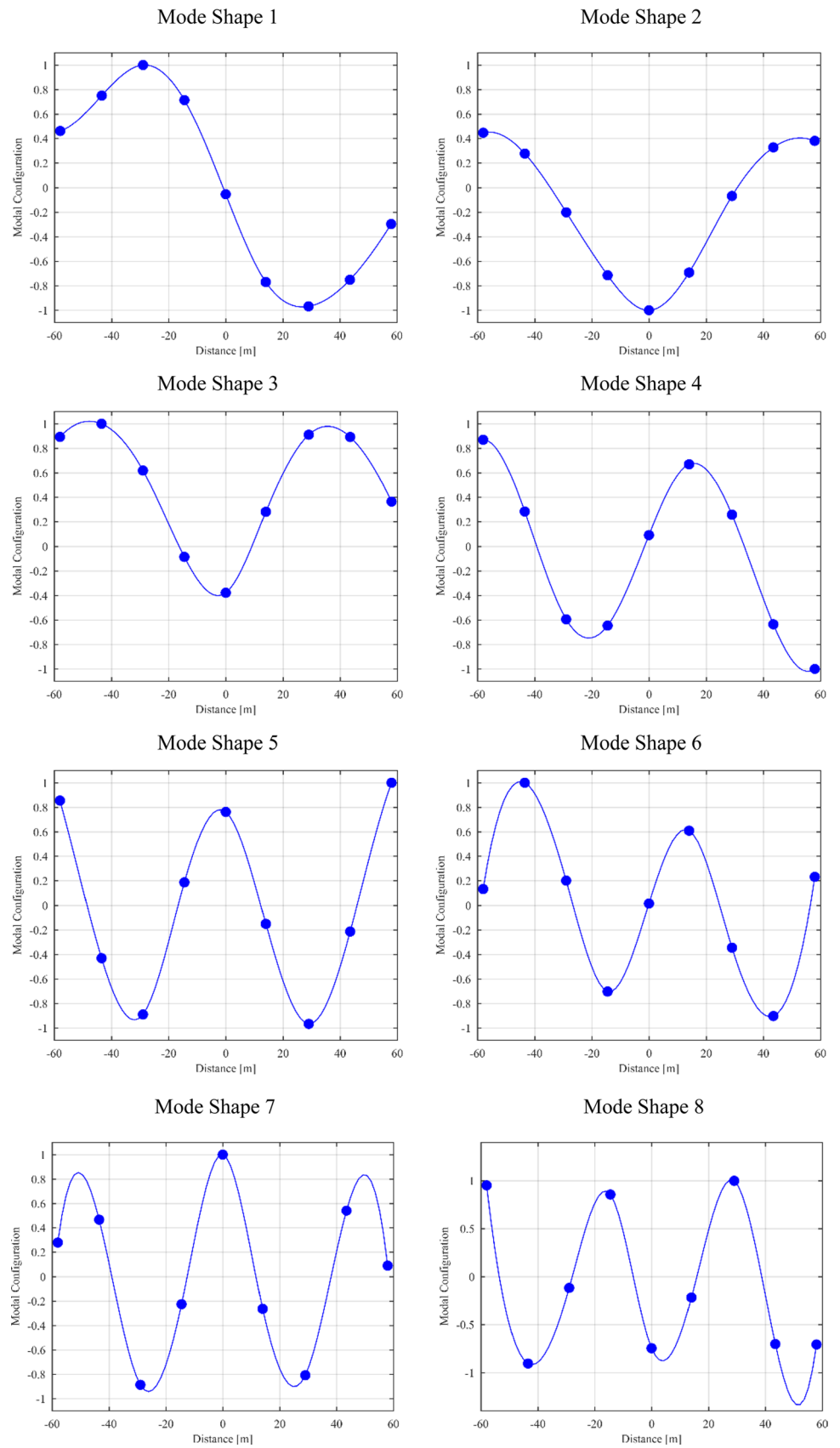
Fig. 17 **a**: auto-spectra from real data (blue) and auto-spectra from noise floors numerically generated; **b**: auto-spectra from real data added to numerically generated noises

The auto-spectra obtained from real data measured in Bouçã dam with force-balance sensors (in blue) and the auto-spectra that resulted from the four scenarios simulating that piezoelectric and MEMS accelerometers were used during the test are presented in Fig. 17b. It is worth noting that only a minor fraction of the peaks in the spectra resulting from the experimental data (FB) are reflected in the spectra resulting from the time-series used to simulate that piezoelectric sensors had been used (PE1 and PE2) during the test. In turn, the 'MEMS' derived spectra do not seem to distinctly show any peak at all, which lay unknown below the noise floors (Fig. 18).

Such as in the case of Alto Lindoso dam, an automatic operational modal analysis was performed resorting to the application of the SSI-Cov method to the time-series of

accelerations available for the five scenarios under study (FB, PE1, PE2, MEMS1, and MEMS2).

The modal properties obtained for the first two vibrations modes of the structure through the study of each of the studied scenarios are presented in Table 5, including mean and standard deviations values of natural frequencies and damping ratios. As was expected, the analysis of Table 5 reflects a relationship between the amplitude of uncertainties and the level of noise added to the recorded time-series, being that the first increases with the second. For instance, only the second vibration mode could be identified using MEMS, and the standard deviation values associated with modal properties identified are excessively high.
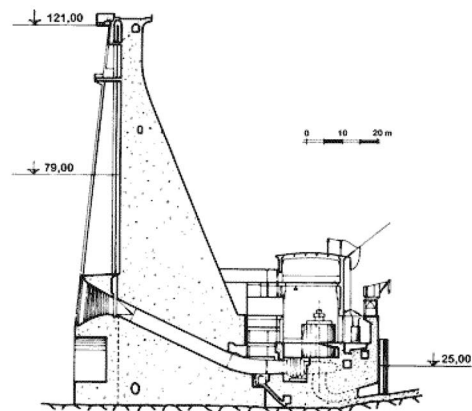

Fig. 18 Aerial view [33] and cross section [50] of Castelo do Bode dam

Table 5 Natural frequencies, damping ratios, and corresponding standard deviations for the first two vibration modes of Buçã dam

Scenario	f_{mean}[Hz]	f_{std}[Hz]	ξ_{mean}[%]	ξ_{std} [%]
Mode 1				
FB	3.2960	0.0069	1.464	0.206
PE1	3.3010	0.0157	1.544	0.438
PE2	3.2910	0.0185	1.554	0.528
MEMS1	–	–	–	–
MEMS2	–	–	–	–
Mode 2				
FB	3.7330	0.0058	1.308	0.161
PE1	3.7350	0.0082	1.228	0.283
PE2	3.7380	0.0113	1.340	0.383
MEMS1	3.7470	0.1281	1.942	2.687
MEMS2	–	–	–	–

6 Castelo do Bode dam

6.1 Description of the dam and ambient vibration test

Castelo do Bode is a concrete arch-gravity dam located between Tomar and Abrantes, in Portugal, whose reservoir is accomplished with water from the Zêzere River. The 115-m-high and 402-m-long dam is operating since 1951 when three vertical Francis turbines working at 214.3 rpm (3.57 Hz) where installed in the hydroelectric plant that lays at the downstream foot of the dam. Figure 16 presents an aerial picture of the dam, side-by-side with a scheme of the cross section.

On the 17th of July 2018, an ambient vibration test was realized on Castelo do Bode dam. Since the dam's crown is too large to be covered using sensors connected to a central acquisition system, ten portable recorders (model GSR-24 from Geosig) where used to perform the test, which remained in the same position during the entire

experimental campaign, given that enough sensors were available.

Measuring points were selected, so that every two consecutive concrete blocks at least one of them had a sensor recording data, with the exception being the two spillway blocks where two sensors were positioned, to characterize this particular part of the structure better. All accelerometers were positioned in the middle of a concrete block. The test layout is presented in Fig. 19 using a scheme of the structure and red dots to point the position of each measuring point. The test consisted of eight recording setups, each of them with 13 min of duration, and the data acquisition was performed with a sampling rate of 100 Hz (reduced to 50 Hz during pre-processing). The elevation of the water in the reservoir throughout the experimental procedures was constant at 116.6 m.

6.2 Identification of modal properties

Once again, the identification of modal properties started with the application of the Peak-Picking method. Autospectra and averaged normalized power spectral density functions (ANPSD) were obtained and analysed. The latter is presented in Fig. 20.

Since the turbines in the power station operated during the entire test, parasite frequencies corresponding to their rotation frequency (214 rpm ~ 3.57 Hz) and their harmonics are observable in the spectra resulting from all the data series recorded in the dam. This is the case of the first observable peak present in Fig. 20, which is very thin. On the other hand, it is hard to distinguish the peak of the first harmonic (7.14 Hz) in the ANPSD function.

Afterwards, the SSI-Cov method was used to confirm and improve the identification of the dam's modal properties and similar stabilization diagrams resulted from the analysis of the time-series recorded during the entire test. Figure 21 shows the stabilization diagram obtained from data recorded during the third setup, where blue lines were adopted to point the alignments related to the vibration
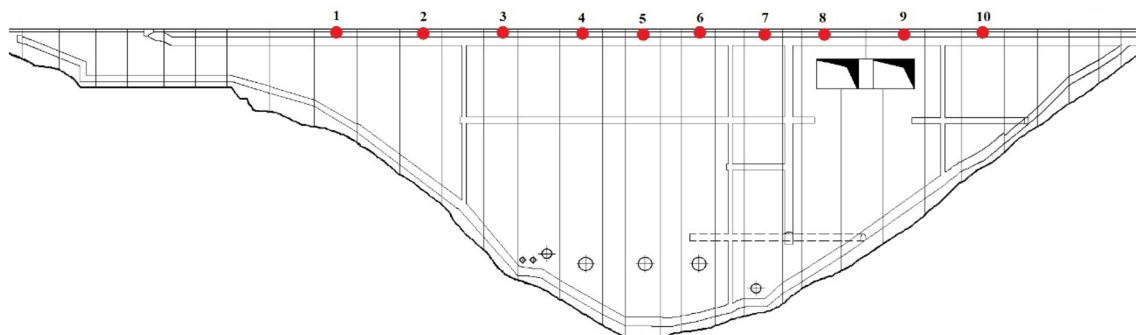

Fig. 19 Castelo do Bode dam: test layout

modes determined. Comparing the stabilization diagram in Fig. 21 with those presented in Figs. 9, 15, it can be observed that in the case of Castelo do Bode dam, except for the first and second vibration modes, higher model orders had to be used until clear and stable vertical alignments of poles were formed. Therefore, model orders between 70 and 150 were considered during the application of SSI-Cov method.

Finally, it is relevant to note that the entire set of peaks and alignments observed, respectively, in the power spectral density function and the stabilization diagram were investigated, which included the analysis of the shapes of the modal configurations resulting from all of them. The group of identified vibration modes settled at the end of the analysis corresponds to the ones that were achieved simultaneously through the two identification methods, and that presented reasonable mode shapes as well.

The modal properties of the five vibration modes identified are presented in Table 6. The presented values result from the averaging of the results obtained from the selected stable poles for the recorded setups.

Besides the estimates of the mean values, also standard deviations are presented for natural frequencies and damping ratios in Table 6, which give extra information on the accuracy of the estimates obtained.

It is relevant to note that the 3rd and 4th modes, which needed higher model orders before getting stabilized (see Fig. 21), coincide with the modes presenting higher standard deviations values for natural frequencies, out of the identified vibration modes. Contrarily, the lower standard deviation estimate is associated with the 2nd mode of vibration, which presents a steady arrangement of poles from much lower model orders.

Fig. 20 ANPSD function obtained from data recorded during the experimental campaign carried out at Castelo do Bode dam, with orange circles highlighting the identified vibration modes
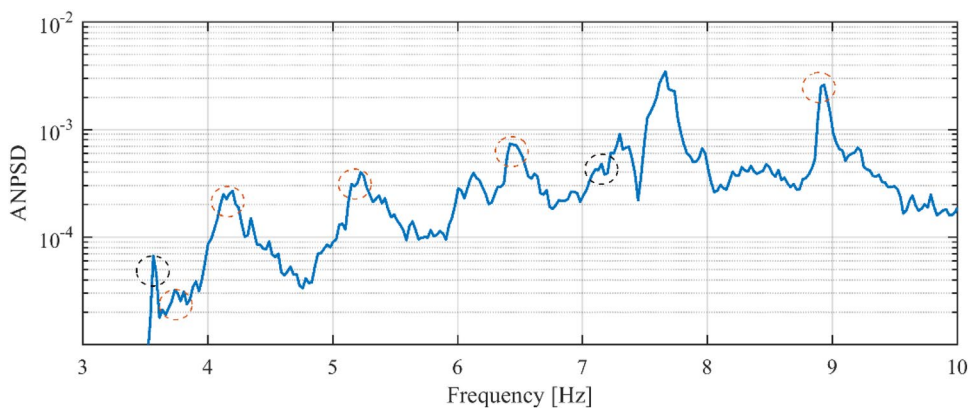

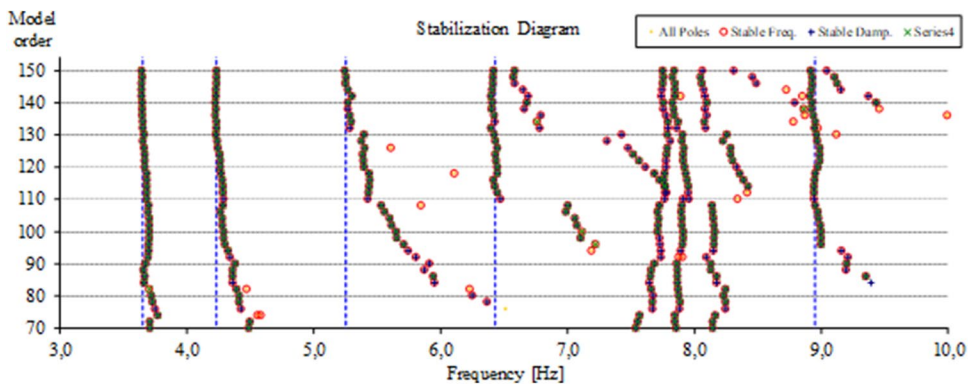**Fig. 21** Castelo do Bode arch dam stabilization diagram

Table 6 Modal properties of Castelo do Bode

| Mode order	f_{mean}[Hz]	f_{std}[Hz]	ξ_{mean}[%]	ξ_{std} [%]	Mode shape description
1st	3.6480	0.0204	6.415	0.621	Global
2nd	4.2300	0.0145	3.273	0.313	Left side of the spillway
3rd	5.2360	0.0326	3.069	0.639	Global
4th	6.4300	0.0409	2.188	0.648	Left side of the spillway
5th	8.9500	0.0289	1.300	0.418	Left side of the spillway

The dam's asymmetric nature and the additional stiffness granted by the two elements used for water discharge (see the spillways picture and scheme in Figs. 18, 19) create conditions for the occurrence of local vibration modes, which result in mode shapes with very close modal ordinates near the spillway. In contrast, the other half of the mode configuration match the traditional shapes, presenting a count of geometric inflexions that increase between consecutive modes.

Regarding the global modes identified and their shapes, the two traditional configurations, presenting either one or two geometric inflexions, could not be identified.

Furthermore, an identical mode shape to that of the 1st mode (3.648 Hz) was found with a frequency of about 8 Hz. This may be related with a mode of higher order presenting a similar shape at the top of the dam, yet distinctly developing at lower regions of the dam. Consequently, it would have been necessary to synchronously record data in the structure's galleries, so that this mode could be undoubtedly identified and included in the results presented.

Figure 22 presents the modal configurations of the five vibration modes identified. Global modes are associated with vibration modes 1 and 3, while the other three vibration modes are related to the deflection of the left part of the structure.

Fig. 22 Castelo do Bode dam: mode shapes of the identified vibration modes
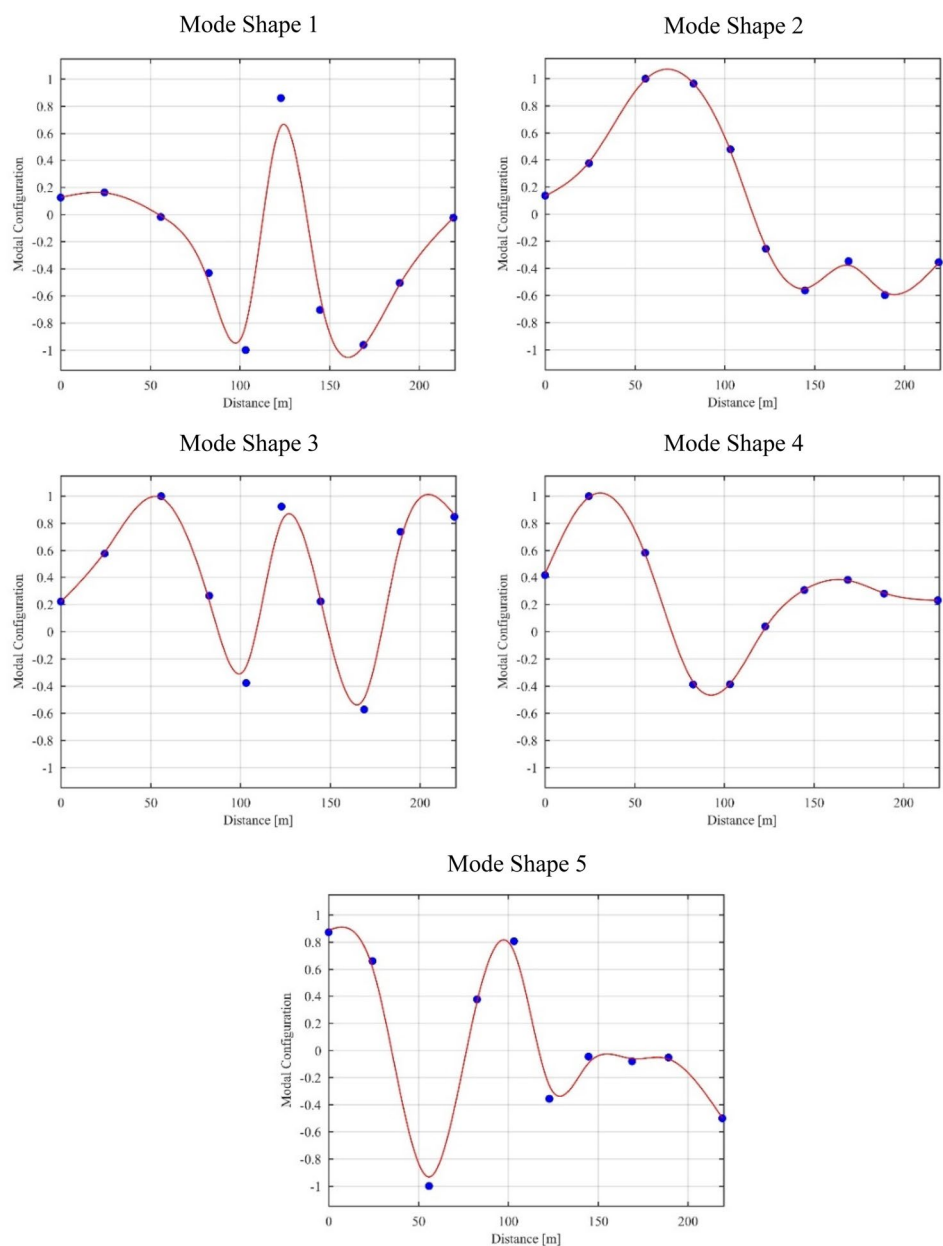
7 Other tested dams

The procedures followed during the tests presented before, and the subsequent data processing were used as well in the tests and modal properties identification of Caldeirão, Santa Luzia, and Aguieira dams. The results obtained for these three dams are summarized in this section. More information about the tests performed on these dams can be found in [53].

Natural frequencies and damping ratios for the first two vibration modes identified in each test are presented in Table 7. In addition, the values of reservoir level (above sea level) and the values of turbine rotation frequency in the power plants near each dam are presented as well, since they influence modal properties and the modal identification process, respectively.

The damping ratios obtained for the first two identified vibration modes generally present values between 1.5 and 2.1% for the three dams (with the exception being the second mode of Caldeirão dam). In the case of natural frequencies, however, quite different values were obtained for Santa Luzia and Aguieira dams when compared with Caldeirão dam, which present natural frequencies above 12 Hz for the first two modes, showing how stiff the structure is.

Finally, mode shapes for the first two identified modes of each dam are presented in Fig. 23. Identical mode shapes were found in the cases of Caldeirão and Santa Luzia dams, while in the case of Aguieira dam, which is composed by three arches, more complex shapes are obtained, since the complete shape results from the sum of each arches' individual shape.

Table 7 Modal properties of the first two identified modes and test conditions

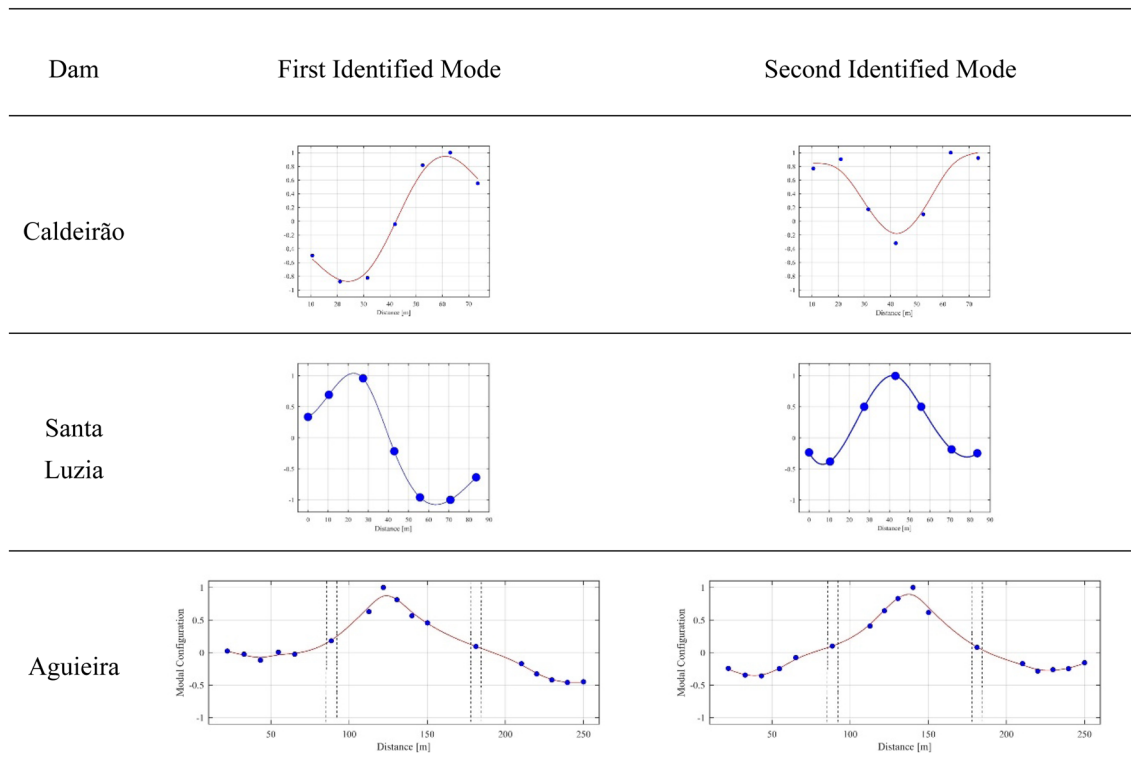| Dam	First mode		Second mode		Reservoir level [m]	Turbine rotation frequency [rpm]
	Frequency [Hz]	Damping [%]	Frequency [Hz]	Damping [%]		
Caldeirão	12.265	2.074	15.759	0.336	699.9	333.3
Santa Luzia	4.910	1.694	6.596	1.870	655.1	500
Aguieira	3.956	1.910	4.368	1.886	123.6	125

Fig. 23 Mode shapes of the first two identified modes

8 Conclusions

Experimental campaigns relying solely on excitation from the surrounding environment have been conducted in a set of six Portuguese concrete dams with quite diverse structural characteristics and the data collected used to identify their modal properties, demonstrating that it is appropriate to use operational modal analysis to the study of concrete dams. The tests were performed under diversified operational conditions, occasionally incorporating excitation due to electricity production turbines rotating in nearby hydroelectric developments. The tested structures include four-arch dams with quite contrasting dimensions, one arch-gravity dam, and one multiple arch dam.

Each dam was tested with (at least) one of the two acquisition systems available, which was chosen for each case regarding the geometrical characteristics of the structure. Most of the tests were conducted in the dam's crowns, commonly of easy access and consisting of road connecting the two margins of a river. The test performed in Bouçã dam was the exception, since the crown of the dam corresponds to its main spillway, which is not accessible, forcing the test to be performed in the first visit gallery.

The excitation to which dams are subjected may vary significantly from one to the next and even on the same structure depending on the hour of the day. In the cases where there is a power plant in the vicinity of the dam, the intensity of the vibrations recorded may increase 100–1000 times due to the operation of the turbines, thus varying from few micro g to few milli g. This effect was recorded in all the tested dams, except for Santa Luzia dam, whose production complex is located afar from the dam.

Finally, a few conclusions can be drawn to sum up the work developed:

- Six concrete dams with quite distinct characteristics were submitted to dynamic tests, and it was concluded that operational modal analysis is suited for the testing of these types of structures.
- Generally, relatively low levels of vibration should be expected, though the proximity to an active power plant may significantly alter this outcome and lead to contamination of the data recorded with the turbine's rotation frequencies and their multiples.
- Ideally, to guarantee quality results, force-balance accelerometers should be used during the performance of ambient vibration tests, though piezoelectric ones seem to be suited, as well. On the other hand, MEMS accelerometers are not likely to provide good results.

References

1. Gauron O, Boivin Y, Ambroise S, Saidou Sanda A, Bernier C, Paultre P, Proulx J, Roberge M, Roth S-N (2018) Forced-vibration tests and numerical modeling of the Daniel-Johnson multiple-Arch Dam. J Perform Constr Facil 32(2):04017137
2. Ellis BR, Jeary AP (1984) On the forced vibration testing of dams. Proceedings of the 8th World Conference on Earthquake Engineering (WCEE), San Francisco, Calif., 5:119–126
3. Paultre P, Proulx J, Carbonneau C (2002) An experimental evaluation of ice cover effects on the dynamic behaviour of a concrete gravity dam. Earthquake Eng Struct Dynam 31(12):2067–2082
4. Gomes JP, Lemos JV (2020) Characterization of the dynamic behavior of a concrete arch dam by means of forced vibration tests and numerical models. Earthquake Eng Struct Dynam 49(7):679–694
5. Bukenya P, Moyo P, Beushausen H, Oosthuizen C (2014) Health monitoring of concrete dams: a literature review. J Civil Struct Health Monit 4(4):235–244
6. Salawu OS, Williams C (1995) Bridge assessment using forced-vibration testing. J Struct Eng (United States) 121(2):161–173
7. Kurata N, Kobori T, Takahashi M, Ishibashi T, Niwa N, Tagami J, Midorikawa H (2000) Forced vibration test of a building with semi-active damper system. Earthquake Eng Struct Dynam 29(5):629–645
8. Gomes J, Pereira S, Magalhães F, Lemos JV, Cunha Á (2018) Input-output vs output-only modal identification of Baixo Sabor concrete arch dam, in 9th European Workshop on Structural Health Monitoring. Manchester, United Kingdom
9. Cunha A, Caetano E, Delgado R (2001) Dynamic tests on large cable-stayed bridge. J Bridge Eng 6(1):54–62
10. Brownjohn JMW, Magalhaes F, Caetano E, Cunha A (2010) Ambient vibration re-testing and operational modal analysis of the Humber Bridge. Eng Struct 32(8):2003–2018
11. Wei-Hua H (2012) Operational modal analysis and continuous dynamic monitoring of footbridges. Faculty of Engineering of University of Porto
12. Magalhães F, Caetano E, Cunha Á, Flamand O, Grillaud G (2012) Ambient and free vibration tests of the Millau Viaduct: evaluation of alternative processing strategies. Eng Struct 45:372–384
13. Magalhães F, Caetano E, Cunha Á (2008) Operational modal analysis and finite element model correlation of the Braga Stadium suspended roof. Eng Struct 30(6):1688–1698
14. Gentile C, Ubertini F, Cavalagli N, Guidobaldi M, Materazzi AL, Saisi A (2014) Dynamic investigation of the "san Pietro" bell-tower in Perugia. In Proceedings of the International Conference on Structural Dynamic, EURODYN
15. Oliveira G, Magalhães F, Cunha Á, Caetano E (2016) Development and implementation of a continuous dynamic monitoring system in a wind turbine. J Civil Struct Health Monit 6(3):343–353
16. Shi W, Shan J, Lu X (2012) Modal identification of Shanghai World Financial Center both from free and ambient vibration response. Eng Struct 36:14–26

17. Furtado A, Rodrigues H, Arêde A, Varum H (2017) Modal identification of infill masonry walls with different characteristics. Eng Struct 145:118–134

18. Nour A, Cherfaoui A, Gocevski V, Léger P (2016) Probabilistic seismic safety assessment of a CANDU 6 nuclear power plant including ambient vibration tests: case study. Nucl Eng Des 304:125–138

19. Magalhães F, Cunha A (2011) Explaining operational modal analysis with data from an arch bridge. Mech Syst Signal Proc 25(5):1431–1450

20. Pereira S, Magalhães F, Gomes JP, Cunha Á, Lemos JV (2018) Dynamic monitoring of a concrete arch dam during the first filling of the reservoir. Eng Struct 174:548–560

21. Deinum PJ, Dungar R, Ellis BR, Jeary AP, Reed GAL, Severn RT (1982) Vibration tests on emosson arch dam, Switzerland. Earthquake Eng Struct Dynam 10(3):447–470

22. Clough RW, Ghannat Y, Qui XF (1987) Dynamic reservoir interaction with Monticello Dam. Earthquake Engineering Research Center

23. Hall JF (1988) The dynamic and earthquake behaviour of concrete dams: review of experimental behaviour and observational evidence. Soil Dynam Earthquake Eng 7(2):58–121

24. Darbre GR, De Smet CAM, Kraemer C (2000) Natural frequencies measured from ambient vibration response of the arch dam of Mauvoisin. Earthquake Eng Struct Dynam 29(5):577–586

25. Proulx J, Paultre P, Rheault J, Robert Y (2001) An experimental investigation of water level effects on the dynamic behaviour of a large arch dam. Earthquake Eng Struct Dynam 30(8):1147–1166

26. Sevim B, Altunisik AC, Bayraktar A (2013) Structural identification of concrete arch dams by ambient vibration tests. 1. En

27. Calcina SV, Eltrudis L, Piroddi L, Ranieri G (2014) Ambient vibration tests of an arch dam with different reservoir water levels: experimental results and comparison with finite element modelling. Sci World J 2014

28. García-Palacios JH, Soria JM, Díaz IM, Tirado-Andrés F (2016) Ambient modal testing of a double-arch dam: the experimental campaign and model updating. J Phys: Conference Series 744(1)

29. Abdulamit A, Demetriu S, Aldea A, Neagu C, Gaftoi D (2017) Ambient vibration tests at some Buttress Dams in Romania. Procedia Engineering 199:2196–2201

30. Gomes JP, Palma J, Magalhães F, Pereira S, Monteiro G, Silva Matos D (2018) Seismic monitoring system of baixo sabor scheme for structural dynamic behaviour monitoring and risk management. In 26th International Congress on Large Dams, 2018

31. Oliveira S, Alegre A (2020) Seismic and structural health monitoring of Cabril dam. Software development for informed management. J Civil Struct Health Monit 10(5):913–925

32. Pacheco J, Oliveira G, Magalhães F, Moutinho C, Cunha Á (2018) Evaluation of low cost vibration based damage detection systems. J Phys: Conf Ser 1037(5):052005

33. EDP, E.d.P. 23/01/2017; http://www.a-nossa-energia.edp.pt/centros_produtores/

34. Santos N, Colaço A, Costa PA, Calçada R (2016) Experimental analysis of track-ground vibrations on a stretch of the Portuguese railway network. Soil Dynam Earthquake Eng 90:358–380

35. Maia N, Silva J (1997) Theoretical and experimental modal analysis. Research Studies Press Ltd

36. Magalhães F (2010) Operational modal analysis for testing and monitoring of bridges and special structures. Faculdade de Engenharia da Universidade do Porto

37. Cantieni R (2005) Experimental methods used in system identification of civil engineering structures. In Proceedings of the 1st International Operational Modal Analysis Conference, IOMAC 2005

38. Oliveira G, Magalhães F, Cunha Á, Caetano E (2018) Continuous dynamic monitoring of an onshore wind turbine. Eng Struct 164:22–39

39. Qu C-X, Yi T-H, Zhou Y-Z, Li H-N, Zhang Y-F (2018) Frequency identification of practical bridges through higher-order spectrum. J Aerospace Eng 31(3):04018018

40. Rainieri C, Fabbrocino G (2014) Operational modal analysis of civil engineering structures, vol 142, Springer, New York, pp 143

41. Reynders E (2012) System identification methods for (operational) modal analysis: review and comparison. Arch Comput Methods Eng 19(1):51–124

42. Qu C-X, Yi T-H, Li H-N (2019) Mode identification by eigensystem realization algorithm through virtual frequency response function. Struct Control Health Monit 26(10):e2429

43. Bendat JS, Piersol AG (1980) Engineering applications of correlation and spectral analysis. John Wiley & Sons, New York

44. Peeters B, De Roeck G (1999) Reference-based stochastic subspace identification for output-only modal analysis. Mech Syst Signal Proc 13(6):855–878

45. Reynders E, Pintelon R, De Roeck G (2008) Uncertainty bounds on modal parameters obtained from stochastic subspace identification. Mech Syst Signal Proc 22(4):948–969

46. Döhler M, Mevel L (2013) Efficient multi-order uncertainty computation for stochastic subspace identification. Mech Syst Signal Proc 38(2):346–366

47. Pereira S, Reynders E, Magalhaes F, Cunha A, Gomes J (2020) The role of modal parameters uncertainty estimation in automated modal identification, modal tracking and data normalization. Engineering Structures

48. Qu C-X, Mei D-P, Yi T-H, Li H-N (2018) Spurious mode distinguish by modal response contribution index in eigensystem realization algorithm. Struct Design Tall Special Buildings 27(12):e1491

49. Evans JR, Allen RM, Chung AI, Cochran ES, Guy R, Hellweg M, Lawrence JF (2014) Performance of several low-cost accelerometers. Seismol Res Lett 85(1):147–158

50. CNPGB, C.N.P.d.G.B.; http://cnpgb.apambiente.pt/gr_barragens/gbportugal/Lista.htm

51. Câmara R, Oliveira S, Portugal A (1993) Estudo do comportamento dinâmico da barragem do Alto Lindoso

52. Westergaard HM (1835) Water pressures on dams during earthquakes. Trans ASCE 1933(98):418–433

53. Pereira S (2019) Structural condition assessment of dams based on continuous dynamic monitoring. Faculty of Engineering of University of Porto: Porto. English

Publisher's Note Springer Nature remains neutral with regard to jurisdictional claims in published maps and institutional affiliations.